

# System analysis of multilane traffic flow models with different lane changing motivations

D. A. PESTOV<sup>1,2</sup>, M. N. SMIRNOVA<sup>1</sup>, V. F. NIKITIN<sup>1,2</sup>, V. V. TYURENKOVA<sup>1,2</sup>, ZUOJIN ZHU<sup>3</sup>

1. Faculty of Mechanics and Mathematics, Moscow M.V.Lomonosov State University, Moscow, RUSSIA
2. Federal Science Center “Scientific Research Institute for System Analysis”, Russian Academy of Sciences, Moscow, RUSSIA
3. Faculty of Engineering Science, USTC, Hefei, 230026, CHINA  
marija\_smirnova@lenta.ru

**Abstract** – The present research was aimed at mathematical modeling of essentially unsteady-state traffic flows on multilane roads, wherein massive changing of lanes produces an effect on handling capacity of the road segment. The model takes into account drivers’ motivations for lane changing before the crossing caused by the necessity of the maneuver on entering multilane road crossing. The model is based on continua approach. However, it has no analogue in the classical hydrodynamics because momentum equations in the direction of a flow and in orthogonal directions of lanechanging are different. To provide stability and accuracy of the numerical solution we use the computation method common to gas dynamics. Numerical simulations of traffic flows in multilane roads were performed and their results are presented.

**Keywords** – continuum, traffic, flow, model, two-dimensional, anisotropy, multi-class, multilane road, AUSM scheme

## 1. Introduction

Traffic flows have been widely studied due to significant impacts on economic activities and travel time. Therefore, many macroscopic traffic models have been developed to define characteristics and properties of traffic flows, for instance, the LWR model [1, 2], the Euler model [3], the gas-kinetic-based model [4, 5], the Navier-Stokes like model [6], the class of second order models [7, 8], and the generic model [9, 10].

Greenberg [7,11] analyzed a class of second-order traffic models and showed that these models support stable oscillatory traveling waves typical of the waves observed on a congested roadway. The stable traveling waves arise as there is an interval of car spacing for which the constant solutions are unstable. These waves consist of a smooth part where both the velocity and spacing between successive cars are increasing functions of a Lagrange mass index.

Borsche, Kimathi and Klar [8] reviewed and numerically compared a special class of

multiphase traffic theories based on microscopic, kinetic and macroscopic traffic models, and found that for all models, but one, phase transitions can appear near bottlenecks depending on the local density and velocity of the flow.

By applying and extending methods from statistical physics and nonlinear dynamics to self-driven many-particle systems, Helbing [12] answered some questions about traffic flows, such as: Why are vehicles sometimes stopped by ‘phantom traffic jams’ even though drivers all

like to drive fast? What are the mechanisms behind stop-and-go traffic? Why are there several different kinds of congestion, and how are they related? etc. Nagatani [13] reported that traffic systems display a surprisingly rich spectrum of spatial-temporal pattern formation phenomena. These phenomena can be explored by using the car-following models [14], the cellular automaton models [15–17]), the gas-kinetic models or the fluid-dynamical models [4–6].

Currently, continuum traffic flow modelling is developing in a number of directions. Some of new models concentrate on the methods of determining the optimal model parameters for the model equations [20-22]. Other developed models taking into account different types of vehicles or different driving styles [23] or models with deeper view on information propagation across the traffic [24]. Another approach using discrete approximation for public traffic and passengers' interaction is illustrated by [25,26]. Finally, some models expanded to two-dimensions to describe the traffic flow on multilane roads [27].

Some notable researches about macroscopic traffic models can be found in Refs. [28–34], with the sensitivity of traffic flow to viscoelasticity reported recently by Smirnova et al. [35, 36]. While for travel time prediction, a relatively detail background has been given in Ref. [37], with some more recent work reported in Refs. [38–41].

The present research was aimed at creating a method for effective modelling of traffic flows on crossroads and road junctions, where massive line-changing significantly affect velocity and density of the flow. Moreover, presented multi-component model can be used to simulate traffic flows consisting of different types of vehicles with different behaviour (cars, trucks, buses etc.).

## 2. The continua model of traffic flows

We introduce Euler's coordinate system with the  $Ox$  axis directed along the auto route and the  $Oy$  axis directed across the traffic flow. Time is denoted by  $t$ . The average flow density  $\rho(x, y, t)$  is defined as the relation of the surface of the road occupied by vehicles to the total surface of the road considered (by the 'occupied surface' we mean the surface physically occupied by the vehicle and the area necessary to keep safe distance between vehicles, the so-called "dynamic clearance"):

$$\rho = \frac{S_{tr}}{S} = \frac{hNl}{HL} = \frac{nl}{L},$$

where  $h$  is the lane width,  $H$  is the sample road width,  $L$  is the sample road length,  $l$  is an average vehicle's length plus a minimal distance between jammed vehicles,  $N$  is the number of vehicles on the road,  $n$  is the mean number of vehicles on the lane. With this definition, the density is dimensionless changing from zero to unit.

The flow velocity denoted  $V(x, y, t) = u(x, y, t), v(x, y, t)$ , where  $u$  can vary from zero to  $U_{max}$ , where  $U_{max}$  is maximal permitted road velocity. From definitions, it follows that the maximal density  $\rho = 1$  relates to the case when vehicles stay bumper to bumper. It is natural to assume that the traffic jam with  $V = 0$  will take place in this case.

Determining the "mass" distributed on a road sample of the area  $S$  as:

$$m = \int_S \rho \, dx dy,$$

one can develop a "mass conservation law" in the form of continuity equation:

$$\frac{\partial \rho}{\partial t} + \frac{\partial(\rho u)}{\partial x} + \frac{\partial(\rho v)}{\partial y} = 0 \quad (1)$$

Then, we derive equation for the traffic dynamics. The traffic flow is determined by different factors: drivers' reaction to the road situation, drivers' activity and vehicles response, technical features of vehicles. The following assumptions were made in order to develop the model:

- It is the average motion of the traffic described and not the motion of individual vehicles, that is modeled. Consequently, the model deals with the mean features of the vehicles not accounting for variety in power, inertia, braking distances, etc.
- The "natural" reaction of all the drivers is assumed. For example, if a driver sees red lights, or a velocity limitation sign, or a traffic hump ahead, he is expected to decelerate until full stop or until reaching a safe velocity, and not to keep accelerating with further emergency braking.
- It is assumed that the drivers are loyal to the traffic rules. In particular, they accept the velocity limitation regime and try to maintain the safe distance depending on velocity.

The velocity equation for the x-component is then written as follows:

$$\frac{du}{dt} = a, \quad a = \max\{-a^-; \min\{a^+, a_x\}\};$$

$$a_x = \sigma a_\rho + \frac{(1-\sigma)}{\Delta} \int_x^{x+\Delta} a_\rho(t, s) \, ds + \frac{U(\rho)-u}{\tau};$$

$$a_\rho = -\left. \frac{k^2 \partial \rho}{\rho \partial x} \right|_+$$

Here,  $a$  is the acceleration of the traffic flow;  $a^+$  is the maximal positive acceleration,  $a^-$  is the emergency braking deceleration;  $a^+$  and  $a^-$  are positive parameters which are determined by technical features of the vehicle. Subscripts plus and minus denote derivative from the right and from the left respectfully. The parameter  $k > 0$  is the small disturbances propagation velocity

(“sound velocity”), as it was shown in [42]. The parameter  $\tau$  is the delay time which depends on the finite time of a driver’s reaction to the road situation and the vehicle’s response. This parameter is responsible for the drivers tendency to keep the vehicles velocity as close as possible to the safe velocity depending on the traffic density  $U(\rho)$ :

$$U(\rho) = \begin{cases} k \ln \rho, & u < U_{max} \\ \min\{U_{max}; k \ln \rho\}, & u \geq U_{max} \end{cases}$$

The velocity  $U(\rho)$  is determined from the dependence of the traffic velocity on density in the “plane wave” when the traffic is starting from the initial conditions  $\rho_0 = 1$  and  $u = 0$ , with account of velocity upper bound ( $u < U_{max}$ ). The value of  $\tau$  could be different for the cases of acceleration or deceleration to the safe velocity  $U(\rho)$ :

$$\tau = \begin{cases} \tau^+, & U(\rho) < u \\ \tau^-, & U(\rho) \geq u \end{cases}$$

In the formula for  $a_x$  the first term describes an influence on the driver’s reaction in a local situation, the second – a situation ahead the flow and the third – a driver’s tendency to drive a car with the velocity which is the safest in each case. If we assume  $\sigma = 0$ , then the expression for  $a_x$  will be:

$$a_x = \frac{1}{\Delta} \int_x^{x+\Delta} a_p(t, S) ds + \frac{U(\rho) - u}{\tau}$$

In this case acceleration is not a local parameter, but depends on its values in the region of length  $\Delta$  ahead of vehicle, where  $\Delta$  - is the distance each driver takes into account on making decisions. This distance depends on road and weather conditions. The last term of the relaxation type takes into account tendency to reach optimal velocity.

If we assume  $\sigma = 1$ , then the expression for  $a'$  will be:

$$a_x = a_p + \frac{U(\rho) - u}{\tau}$$

Now acceleration depends on local situation only.

We will consider a case when  $\sigma = 1, \tau = \infty$ , so the equation of motion for the x-component is:

$$a_x = -\frac{k^2}{\rho} \frac{\partial \rho}{\partial x} \Big|_+ \quad (2)$$

The equation of motion for the y-component we can write in such form as for the x direction:

$$a_y = -\frac{A^2}{\rho} \frac{\partial \rho}{\partial y} \quad (3)$$

The description for parameter A will be given below.

In order to understand the physical meaning of the parameter A we shall consider the following model problem. One car is changing its lane

with the density  $\rho \neq 0$  to the lane with the density  $\rho = 0$ . In this case a car has the maximum acceleration  $a_{max}$ . So by putting  $\frac{\partial \rho}{\partial y} = \frac{0-\rho}{h}$  to the velocity equation for the y-component we can obtain  $\rho \frac{dv}{dt} = -A^2 \frac{\partial \rho}{\partial y}$  and then  $\frac{A^2}{h} = a_{max}$ .

The diagram for the  $v(y)$  is shown in Fig.1. According to it we have:  $v_{max} = \sqrt{a_{max} h}$ , that is  $a_{max} = \frac{v_{max}^2}{h}$  or  $A^2 = v_{max}^2$ . But in this model  $v_{max} = 2v_{av}$  ( $v_{av}$  is an average speed of car's changing a lane), so  $A^2 = 4v_{av}^{max\ 2}$ , where  $v_{av}^{max}$  is the average speed for  $v_{max}$ .

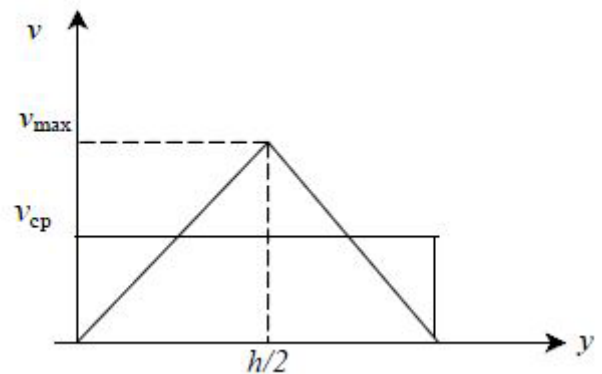


Fig 1: Lane's changing velocity

For the description of lane change dynamics, we approximately assume that the trajectory of maneuver of lane’s changing is assembled of two parts of identical circles (Fig.2). In Fig.2 the bold line is a trajectory of lane’s changing and it begins in the middle of the lane on which the car is going and ends in the middle of the next lane.

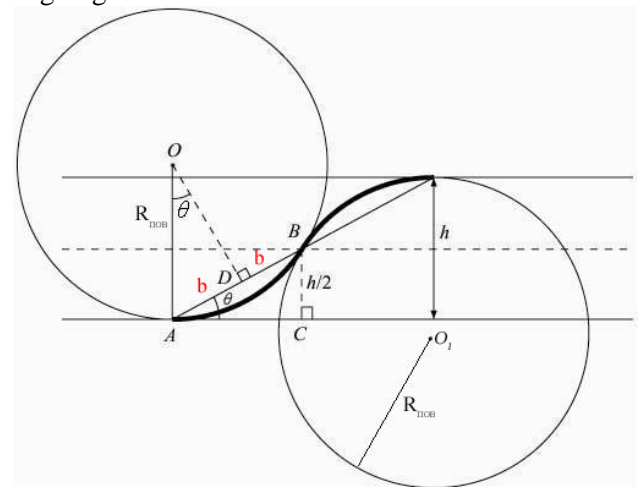


Fig 2: Simplified lane's changing trajectory  
The centripetal force which acts on the car is:  
 $F = \frac{mV^2}{R_{turn}}$ , where  $R_{turn}$  is the radius of the turn,

$V$  - is the velocity of the car, directed by the tangent to the car's trajectory. Let  $F_*$  be the maximum possible flank force under which car is drivable (not skidding),  $F \leq F_*$ . Then we can calculate the radius of the turn  $R_{turn} = \frac{m}{F_*} V^2$ ,  $v_{av}^{max} = V \sin \theta$ . From similar triangles  $\Delta ABC$  and  $\Delta OAD$  (Fig.2) derive that  $AD = DB$ , labeling  $AD = b$  will get:

$$\frac{b}{R} = \frac{h}{4b} \text{ or } b^2 = \frac{Rh}{4},$$

$$\sin \theta = \frac{h}{4b} = \frac{b}{R} = \frac{\sqrt{Rh}}{2R} = \frac{1}{2} \sqrt{\frac{h}{R}}.$$

Then

$$v_{av}^{max} = V \sin \theta = \frac{1}{2} V \sqrt{\frac{h}{R}} = \frac{1}{2} V \sqrt{\frac{h F_*}{m V^2}}$$

$$= \frac{1}{2} \sqrt{\frac{h F_*}{m}}$$

that is the average speed for  $v^{max}$  is  $v_{av}^{max} = \frac{1}{2} \sqrt{\frac{h F_*}{m}}$ . We obtained above  $A^2 = 4 v_{av}^2$ , so the expression for  $A$  is  $A^2 = \frac{h F_*}{m}$ .

Thus we derived parameter  $A^2$  being dependent on the force  $F_*$ , assignable to the lane width, the mass of car and the traction of tires.

The equations (1), (2), (3) provide a system describing traffic flows on multilane roads. Assuming the presence of 3 groups of cars before each crossing characterized by different motivations: going straight, turning left and turning right, one can describe their motivations by introducing different mass forces acting on each group of cars and making them move towards right, central or left lanes, as well as slow down the speed of their motion on approaching the crossing.

$$\frac{\partial \rho_i}{\partial t} + \frac{\partial (\rho u)_i}{\partial x} + \frac{\partial (\rho v)_i}{\partial y} = 0,$$

$$\frac{\partial u}{\partial t} + u \frac{\partial u}{\partial x} + v \frac{\partial u}{\partial y} = - \frac{k^2 \partial \rho}{\rho \partial x} \Big|_+ + g \quad (1)$$

$$\frac{\partial v_i}{\partial t} + u \frac{\partial v_i}{\partial x} + v_i \frac{\partial v_i}{\partial y} = - \frac{A^2 \partial \rho}{\rho \partial y} + f_i$$

$$i = 1, 2, 3; \rho = \rho_1 + \rho_2 + \rho_3,$$

$$v = \frac{1}{\rho} (\rho_1 v_1 + \rho_2 v_2 + \rho_3 v_3).$$

The force slowing down speed before entering crossing has the following model form:

$$g = -(1 - \rho) \frac{U(t) - u}{\tau_0} \exp\left(\frac{x_0 - x}{l_s}\right),$$

where  $l_s$  is the characteristic distance of beginning deceleration in front of the crossing and traffic lights,  $\tau_0$  is characteristic time of reaction to traffic light change.

The forces responsible for the modeling motivation for lane changing could be expressed as follows:

$$f_i = \begin{cases} -(1 - \rho_i) \frac{A^2}{h_i} \exp\left(-\frac{x_0 - x}{l_m}\right), & y > y_i^+ \\ 0, & y_i^+ > y > y_i^- \\ (1 - \rho_i) \frac{A^2}{h_i} \exp\left(-\frac{x_0 - x}{l_m}\right), & y < y_i^- \end{cases} \quad (2)$$

$$y_1^- = 0, y_1^+ = y_2^- = \frac{H}{3}, y_2^+ = y_3^- = \frac{2H}{3}, y_3^+ = H,$$

where  $h_i$  is the respective lane width,  $H$  is the road width.

The system of equations (1) presents a continua model of traffic flow. The term  $-\frac{k^2 \partial \rho}{\rho \partial x}$  was validated long before in the papers [43] by comparing numerical simulation results with experimental data provided in papers [2, 11]. The term  $-\frac{A^2 \partial \rho}{\rho \partial y}$  is a new one, which was accurately derived based on the physical characteristics of vehicles and model assumptions. The form of body forces  $g$  and  $f_i$ , (2) are the assumptions of the model, which should be validated in comparison with experiments. Some independent experimental observations should be used for determining model parameters. For present simulation, we developed model parameters based on the available data. The qualitative comparison of simulation results with the data of direct observations will be provided in the section 4.

### 3. Numerical solution

The problem considered is modelling of car's behaviour on a multilane rectangular road near the crossroad accounting for different maneuvers .at the cross-road planned by the drivers in advance.

#### 3.1. Using AUSM method

The main problem in the numerical solving of the gas-dynamic equations is difference scheme stability. To provide this stability the difference scheme has to contain anti-flow differences [44]. So we have to build scheme taking into account cell interaction and direction of wave

propagation through the grid. In AUSM model interaction between cells is realized by the groups of particles with known velocity distribution. To divide this groups on the ‘flow-oriented’ and ‘anti-flow oriented’ we use the flow splitting methods.

We will solve the following system of equations:

$$\frac{\partial w}{\partial t} + \frac{\partial F}{\partial x} + \frac{\partial G_1}{\partial y} + \frac{\partial G_2}{\partial y} + \frac{\partial G_3}{\partial y} = f,$$

$$w = \begin{pmatrix} \rho_1 \\ \rho_2 \\ \rho_3 \\ \rho u \\ \rho_1 v_1 \\ \rho_2 v_2 \\ \rho_3 v_3 \end{pmatrix}, F = \begin{pmatrix} \rho_1 u \\ \rho_2 u \\ \rho_3 u \\ \rho u^2 + k^2 \rho \\ \rho_1 u v_1 \\ \rho_2 u v_2 \\ \rho_3 u v_3 \end{pmatrix},$$

$$G_1 = \begin{pmatrix} \rho_1 v_1 \\ 0 \\ 0 \\ \rho_1 v_1 u \\ \rho_1 v_1^2 + A^2 \rho \\ 0 \\ 0 \end{pmatrix},$$

$$G_2 = \begin{pmatrix} 0 \\ \rho_2 v_2 \\ 0 \\ \rho_2 v_2 u \\ 0 \\ \rho_2 v_2^2 + A^2 \rho \\ 0 \end{pmatrix},$$

$$G_3 = \begin{pmatrix} 0 \\ 0 \\ \rho_3 v_3 \\ \rho_3 v_3 u \\ 0 \\ 0 \\ \rho_3 v_3^2 + A^2 \rho \end{pmatrix},$$

$$f = \begin{pmatrix} 0 \\ 0 \\ 0 \\ \rho g + \rho \frac{U(\rho)-u}{\tau} \\ \rho_1 f_1 \\ \rho_2 f_2 \\ \rho_3 f_3 \end{pmatrix}.$$

For convenience we denote  $\frac{k^2 \partial \rho}{\rho_i \partial x}$  and  $\frac{A^2 \partial \rho}{\rho_i \partial x}$  as  $p_x$  and  $p_{iy}$  respectively.

The first step to build the AUSM scheme is to divide the flow on convective flow and compressive flow:

$$F = F^c + F^p, \quad G_i = G_i^c + G_i^p,$$

$$M_x = \frac{u}{k}, \quad M_{iy} = \frac{v_i}{A},$$

$$F^c = M_x \begin{pmatrix} \rho_1 k \\ \rho_2 k \\ \rho_3 k \\ \rho u k \\ \rho_1 v_1 k \\ \rho_2 v_2 k \\ \rho_3 v_3 k \end{pmatrix}, F^p = \begin{pmatrix} 0 \\ 0 \\ 0 \\ k^2 \rho \\ 0 \\ 0 \\ 0 \end{pmatrix},$$

$$G_1^c = M_{1y} \begin{pmatrix} \rho_1 A \\ 0 \\ 0 \\ \rho_1 A u \\ \rho_1 A v_1 \\ 0 \\ 0 \end{pmatrix}, G_1^p = \begin{pmatrix} 0 \\ 0 \\ 0 \\ 0 \\ A^2 \rho \\ 0 \\ 0 \end{pmatrix},$$

$$G_2^c = M_{2y} \begin{pmatrix} 0 \\ \rho_2 A \\ 0 \\ \rho_2 A u \\ 0 \\ \rho_2 A v_2 \\ 0 \end{pmatrix}, G_2^p = \begin{pmatrix} 0 \\ 0 \\ 0 \\ 0 \\ 0 \\ A^2 \rho \\ 0 \end{pmatrix},$$

$$G_3^c = M_{3y} \begin{pmatrix} 0 \\ 0 \\ \rho_3 A \\ \rho_3 A u \\ 0 \\ 0 \\ \rho_3 A v_3 \end{pmatrix}, G_3^p = \begin{pmatrix} 0 \\ 0 \\ 0 \\ 0 \\ 0 \\ 0 \\ A^2 \rho \end{pmatrix}.$$

$F^c, G_i^c$ —convective flows,  $F^p, G_i^p$ —compressive flows,  $M_x, M_{yi}$  – Mach numbers. Convective flows are expressed through Mach numbers and column of ‘passive’ values. Compressive flows contain only pressure. Firstly, consider the convective flows. Indexes ‘R’ and ‘L’ denote values on the ‘left’ and ‘right’ of the cells. Convective flows at the cell boundary will be expressed in the following form:

$$F^C = M_x \begin{pmatrix} \rho_1 k \\ \rho_2 k \\ \rho_3 k \\ \rho u k \\ \rho_1 v_1 k \\ \rho_2 v_2 k \\ \rho_3 v_3 k \end{pmatrix}_{L/R},$$

$$G_1^e = M_{1y} \begin{pmatrix} \rho_1 A \\ 0 \\ 0 \\ \rho_1 A u \\ \rho_1 v_1 A \\ 0 \\ 0 \end{pmatrix}_{L/R} \text{ etc.}$$

### 3.2 Splitting the convective flows

The main concept of the AUSM approach is that all flows at the cell boundary are split with

respect to Mach number. It means that all ‘passive’ values transport from the cell from which the flow is directed. We will consider this method in ‘x’ direction. For all flows in ‘y’ direction reasoning is identical up to indexes.

$$M_{xL/R} = \begin{cases} M_{xL}, & M_x \geq 0 \\ M_{xR}, & M_x < 0 \end{cases}$$

We have to split convective velocity  $M_x$  into the ‘left’  $M_{xL}^+$  and ‘right’  $M_{xR}^-$  input. We will search for the functions  $M_{xL}^+$  and  $M_{xR}^-$  satisfying following conditions:

1.  $M_x = M_{xL}^+ + M_{xR}^-$ ;
2.  $M_{xL}^+ \geq 0, M_{xR}^- \leq 0$ ;
3.  $M_{xL}^+(M_x) = -M_{xR}^-(-M_x)$ ;
4.  $M_{xL}^+ = M_x, M_x \geq 1; M_{xR}^- = M_x, M_x \leq -1$ ;
5. Functions are continuous and monotonically increasing;
6. Functions are continuously differentiable

Using the 4<sup>th</sup> condition we obtain the following expression:

$$M_{xL/R}^\pm = \begin{cases} \frac{1}{2}(M_x \pm |M_x|), & |M_x| \geq 1; \\ g(M_x), & |M_x| < 1. \end{cases}$$

Splitting function  $g(M_x)$  is found as least-order polynomial. Using the 6<sup>th</sup> condition and the value of  $M_{xL/R}^\pm$  in case of  $M_x = \pm 1$  we obtain:

$$g^\pm = \pm \frac{1}{4}(M_x \pm 1)^2$$

So we, finally, have

$$M_{xL/R}^\pm = \begin{cases} \frac{1}{2}(M_x \pm |M_x|), & |M_x| \geq 1; \\ \pm \frac{1}{4}(M_x \pm 1)^2, & |M_x| < 1. \end{cases}$$

### 3.3 Splitting the compressive flows

Similarly, pressure  $p_x$  split into ‘left’ and ‘right’ input:

$$p_x = \pi_{xL}^+ + \pi_{xR}^-$$

We will search for functions, which will satisfy the following conditions:

1.  $p_x = \pi_{xL}^+ + \pi_{xR}^-$ ;
2.  $\pi_{xL}^+ \geq 0, \pi_{xR}^- \geq 0$ ;
3.  $\pi_{xL}^+(M_x) = \pi_{xR}^-(-M_x)$ ;
4.  $\pi_{xL}^+ = p_x, M_x \geq 1; \pi_{xR}^- = p_x, M_x \leq -1$ ;
5. Functions are continuous,  $\pi_{xL}^+$  monotonically increases,  $\pi_{xR}^-$  monotonically decreases;
6. Functions are continuously differentiable.

In the same way as for convective flows we obtain the expression to the

$$\pi_{xL/R}^\pm = \begin{cases} \frac{p_x}{2}(1 \pm \text{sign}(M_x)), & |M_x| \geq 1; \\ p_x \pm \frac{1}{4}(M_x \pm 1)^2(2 \mp M_x), & |M_x| < 1. \end{cases}$$

## 4. Solving a test problem

Initially, traffic flow has a density  $\rho = \rho_0$  of which  $\rho_1 = \rho_2 = \frac{\rho_0}{4}, \rho_3 = \frac{\rho_0}{2}$ . The initial velocity of the flow is  $u = u_0, v_1 = v_2 = v_3 = 0$ .

Boundary conditions for  $x=0$ :  $\rho_i u = q_i$

and  $q_1 = q_2 = \frac{q_0}{4}, q_3 = \frac{q_0}{2}$ .

Boundary conditions for  $x=L$  depend on the flow velocity:

if  $u < k, \frac{\partial \rho u}{\partial x} = 0, \frac{\partial \rho_i u_i}{\partial y} = 0, i = 1,2,3$

if  $u \geq k$  there is no boundary condition.

The numerical calculations of the problems were processed using the AUSM method. Other parameters are given below:

The mesh had  $N_x = 201$  and  $N_y = 21$  grid nodes.

$T = 90$  s – calculation time;

$L = 150$  m – the length of the domain;

$H = 10$  m – the width of the domain;

$l_m = 50$  m – characteristic distance of beginning maneuver in front of the crossing;

$l_s = 50$  m – characteristic distance of beginning deceleration in front of the crossing and traffic lights;

$\tau_0 = 3$  s – characteristic time of reaction on traffic light change;

$\rho_0 = 0.01$  – initial density;

$u_0 = 10.0$  m/s – initial velocity of the flow;

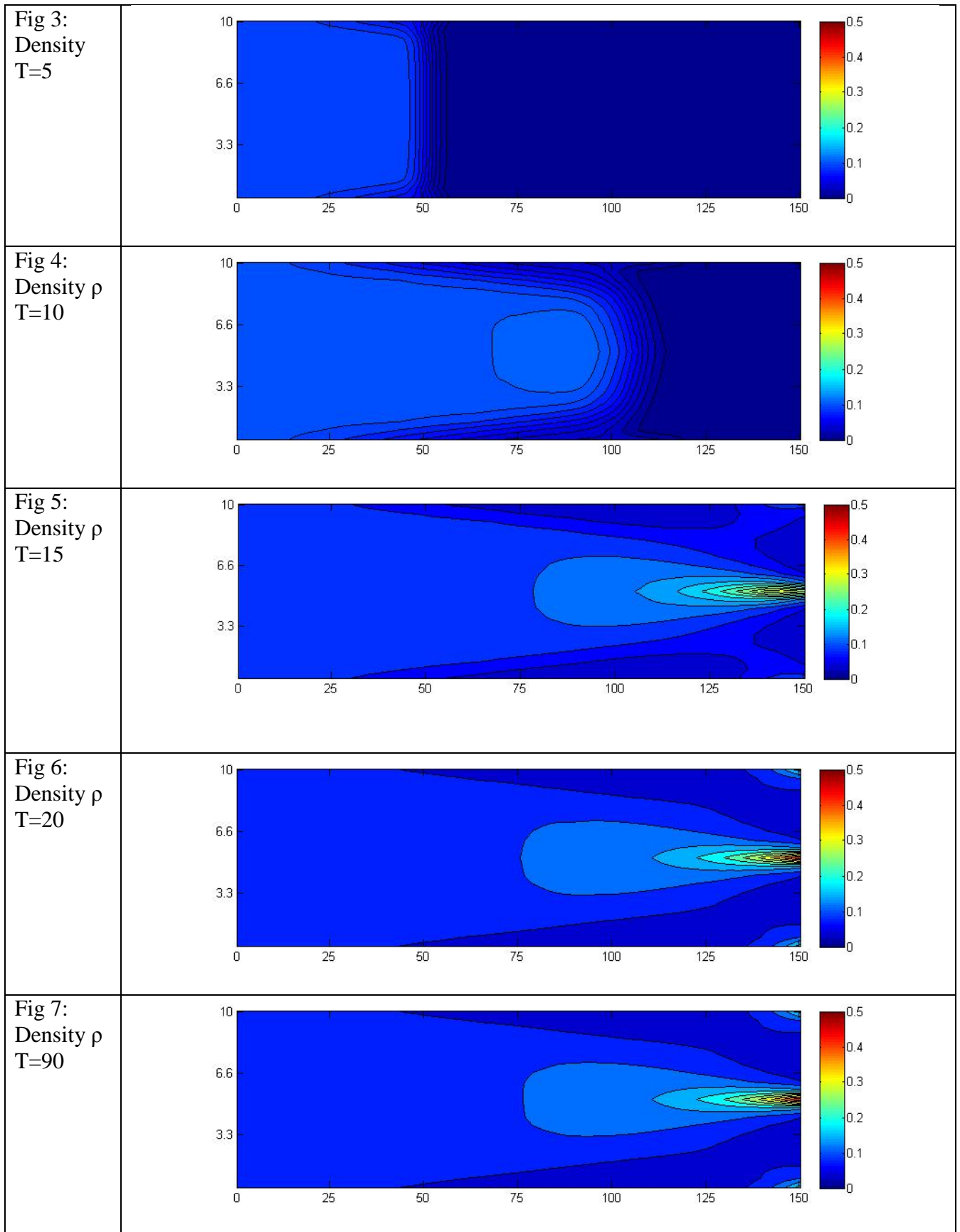
$v_{max} = 20$  m/s – maximal permitted road velocity;

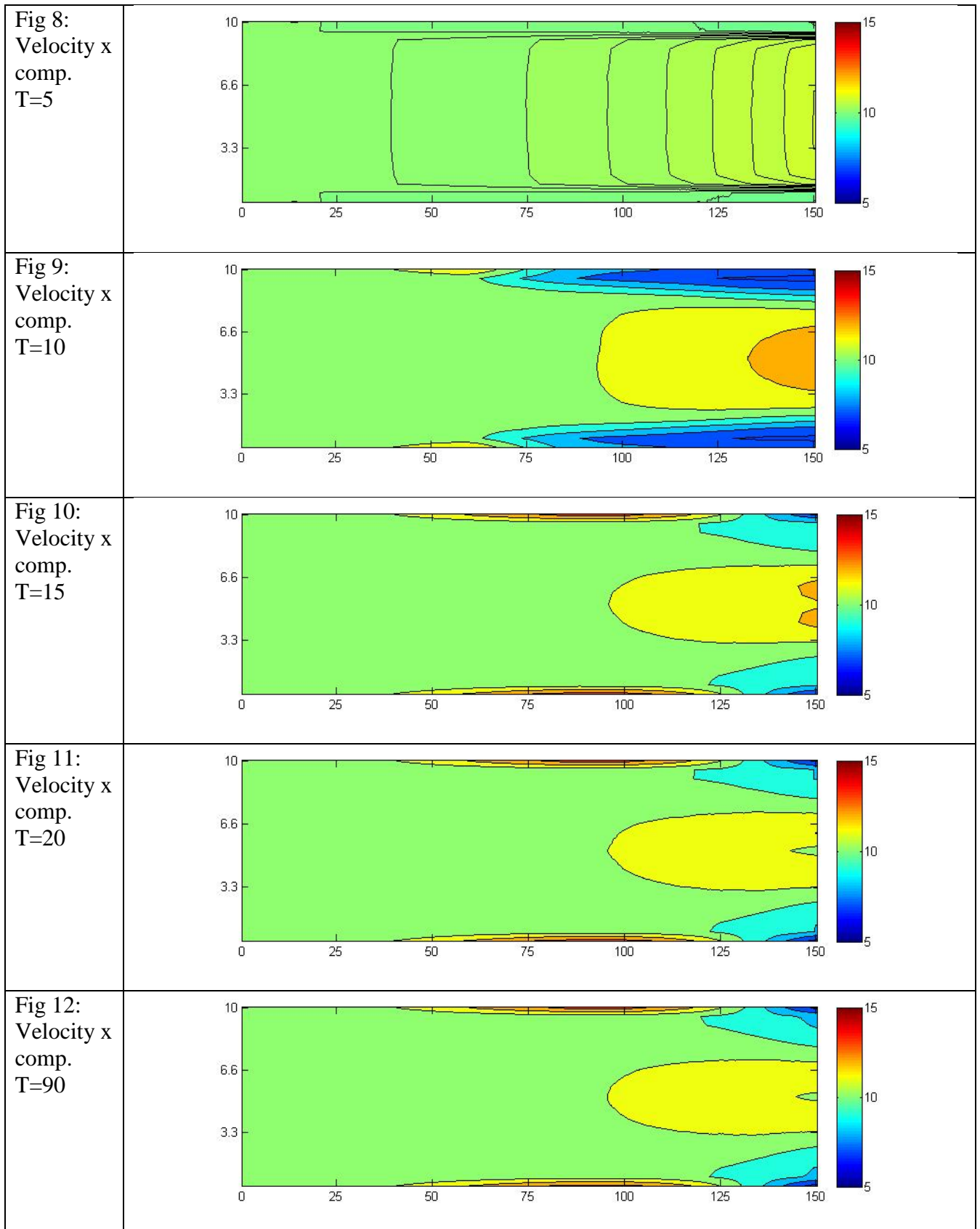
$k = 8$  m/s – the small disturbances propagation velocity (“sound velocity”) on x axis;

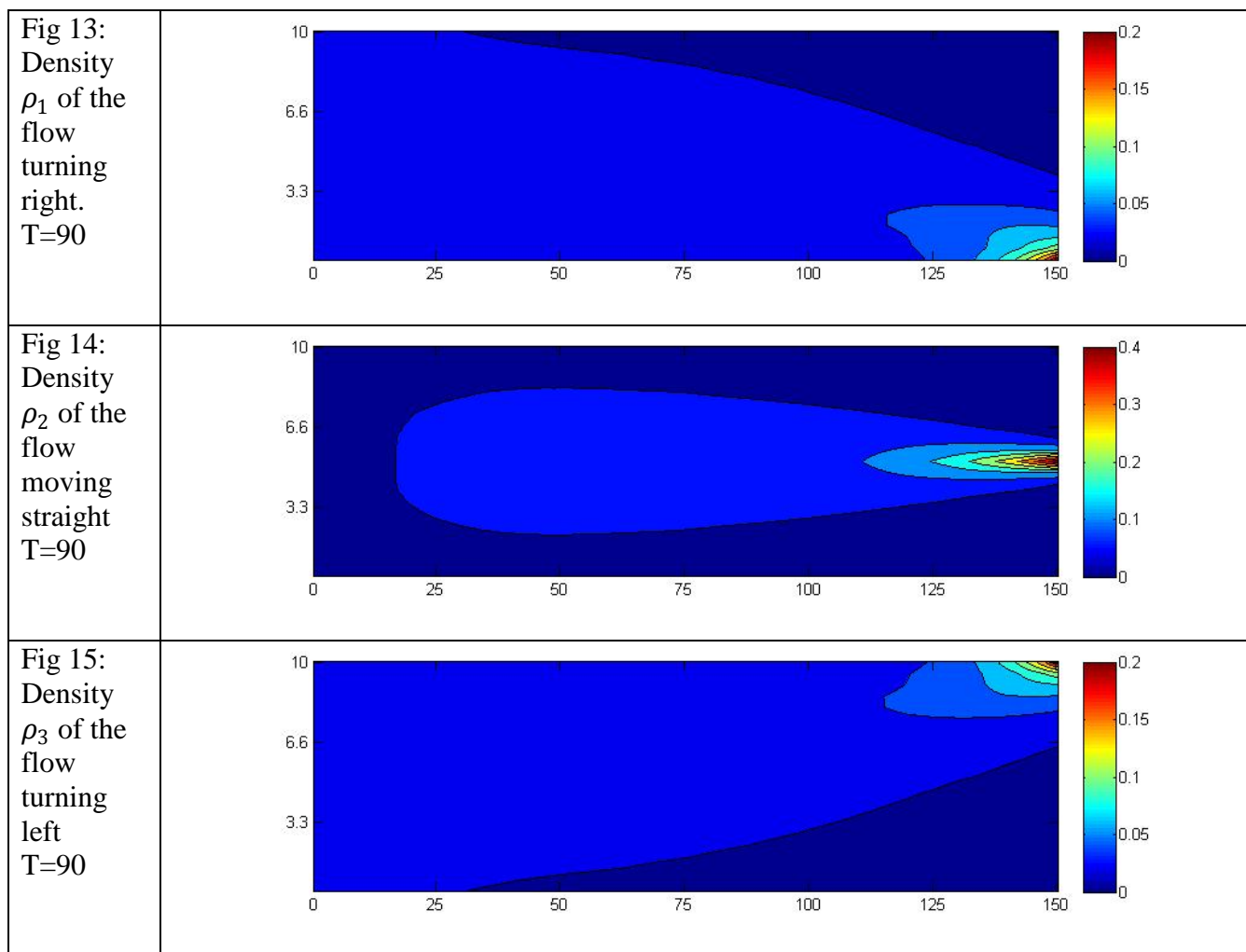
$A = 6$  m/s – the analogy of k coefficient on y axis;

$q_0 = 1$  – a flow on the left boundary.

The results obtained are presented in the form of maps for components of velocity and for density for different moments of time.







As one can see in figures 3-12, the density and the velocity of the flow doesn't change after  $T = 20s$ . This is, approximately, the time it takes to cover the distance  $L$  at speed of  $k$ . Thin areas of increased velocity on figures 10-12 are, apparently, a consequence of decreased density due to changing lanes. Besides, in figures 13-15 one can see densities of each part of the flow. Due to symmetrical initial and boundary conditions the distribution of  $\rho_1$  and  $\rho_3$  are symmetrical to each other.

The qualitative comparison with physical experimental observation can be performed based on result of the vehicles density image taken after some time the turning right and moving straight directions had been open and vehicles passed the crossing, while turning left direction is just open (Fig. 16). As it is seen from Fig. 16 illustrating the 3-lanes road, the vehicles turning left density is concentrated in the left lane near the crossing then gradually spreading to the central and right lanes as it is shown in Fig. 15 for similar conditions.

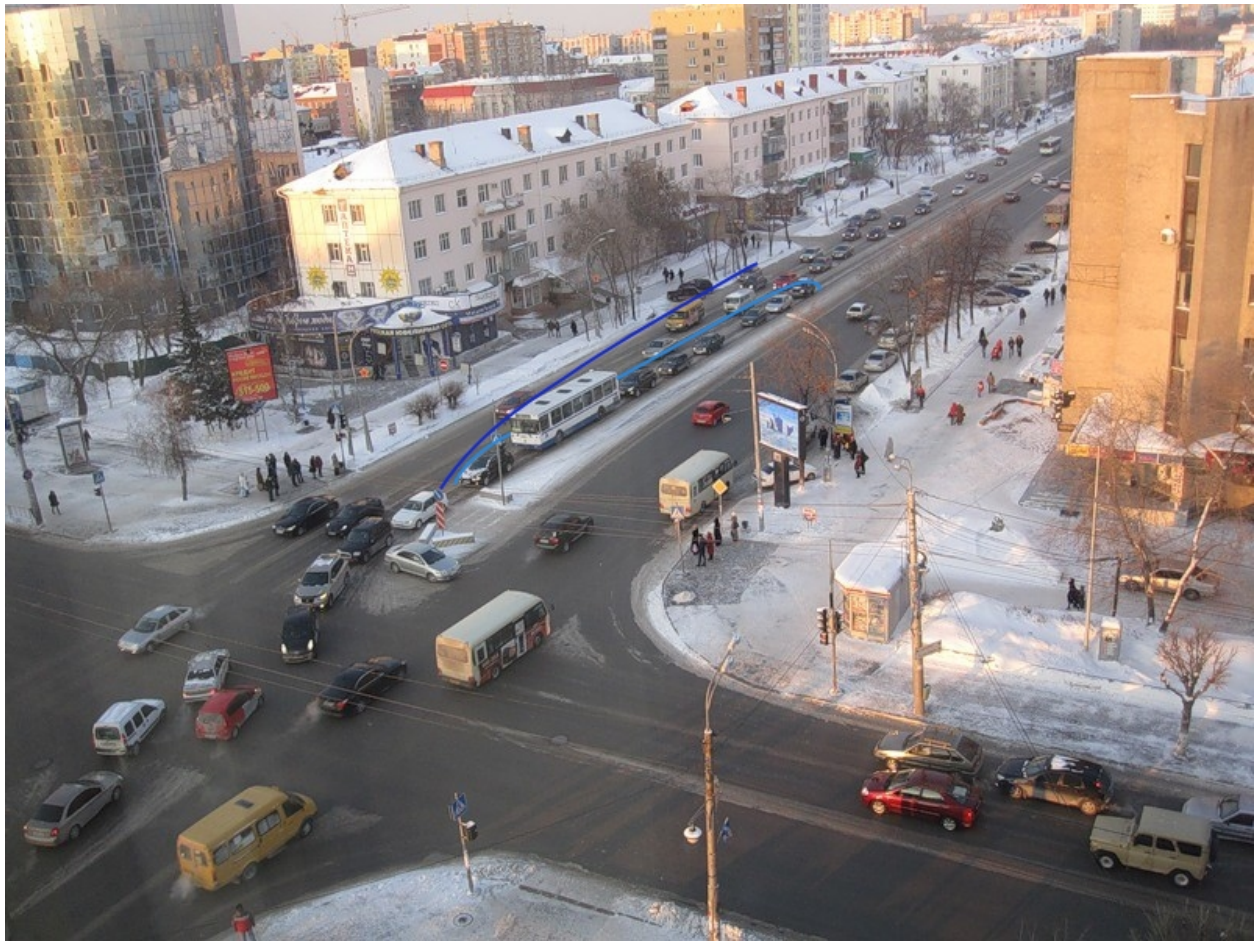


Fig. 16. Image of vehicles turning left density distribution taken after some time the turning right and moving straight directions had been open and vehicles passed the crossing, while turning left direction is just open.

### Conclusions

The mathematical model for traffic flows simulations in multilane roads has been developed. A model problem for traffic evolution in multilane road with different lane changing motivations was regarded. The results show that on exit segment orthogonal fluxes occur in the direction of less dense lanes, which leads to decreasing flow velocity in that lanes and increasing density. This fluxes were counteracted by the lane changing due to driver's motivation. As a result, the flow becomes steady for, approximately, the time needed to cover distance of the test road segment at the speed of small disturbances propagation.

### Acknowledgement

Russian Foundation for Basic Research is acknowledged for financial support (Grant 18-07-00518).

### References

1. Lighthill M.J., Whitham J. On kinetic waves II. A theory of traffic flow on long crowded roads. Proc. of the Royal Society. Ser. A. No. 1178. Vol. 229. London, 1955. 317-345.
2. Richards P.L. Shock waves on the highway. Operations Research. 1956. Vol. 4. 42-51.
3. Payne, H.J. Models of freeway traffic and control. Mathematical Model of Public

- Systems, Simulation Council Proc. La Jola California 1, 51–61(1971)
4. Helbing, D. and Treiber, M. Gas-kinetic-based traffic model explaining observed hysteretic phase transition. *Phys. Rev. Lett.*, **81**, 3042–3045(1998)
  5. Hoogendoorn, S.P. and Bovy, P.H.L. Continuum modeling of multiclass traffic flow. *Transp. Res. Part B*, **34**(2), 123–146(2000)
  6. Kerner, B. S. and Konhäuser, P. Cluster effect in initially homogeneous traffic flow. *Phys. Rev. E*, **48**, 2335–2338(1993)
  7. Greengerg, J.M. Congestion redux. *SIAM J. Appl. Math.*, **64**(4), 1175–1185(2004)
  8. Borsche, R., Kimathi, M. and Klar, A. A class of multi-phase traffic theories for microscopic, kinetic and continuum traffic models. *Computers and Mathematics with Applications*, **64**, 2939–2953(2012)
  9. Lebacque, J.P., Mammari, S. and Haj-Salem, H. Generic second order traffic flow modelling in: *Transportation and Traffic Theory*, edited by R.E. Allsop, and G.H. Benjiamin, Elsevier, Oxford, 755–776(2007)
  10. Lebacque, J.P. and Khoshyaran, M. M. A variational formulation for higher order macroscopic traffic flow models of the gsom family. *Transp. Res. Part B*, **57**, 245–265(2013)
  11. Greenberg H. An analysis of traffic flow. *Operations Research*. 1959. Vol. 7. 79–85.
  12. Helbing, D. Traffic and related self-driven many-particle systems. *Rev. Mod. Phys.*, **73**, 1067–1141(2001)
  13. Nagatani, T. The physics of traffic jams. *Rep. Prog. Phys.*, **65**, 1331–1386(2002)
  14. Brackstone, M., McDonald, M. Car-following: a historical review. *Transp. Res. Part F*, **2**, 181–196(1999)
  15. Nagel, K. and Schreckenberg, M. A cellular automaton model for freeway traffic. *J. De Phys. I*, **2** (12), 2221–2229(1992)
  16. Helbing, D. and Huberman, B.A. Coherent moving states in highway traffic. *Nature*, **396** (6713), 738–740(1998)
  17. Chowdhury, D. Santen, L. and Schadschneider, A. Statistical physics of vehicular traffic and some related systems. *Physics Reports*, **329**, 199–329(2000)
  18. D. Ngoduy, M.J. Maher, Calibration of second order traffic models using continuous cross entropy method, *Transportation Research Part C: Emerging Technologies*, Volume 24, 2012, Pages 102-121, ISSN 0968-090X, <https://doi.org/10.1016/j.trc.2012.02.007>.
  19. Liang Zheng, Zhengbing He & Tian He. An anisotropic continuum model and its calibration with an improved monkey algorithm. *Transportmetrica A: Transport Science* Vol. 13 , Iss. 6, 2017
  20. M. P. Raadsen and M. C. Bliemer. Continuous-time general link transmission model with simplified fanning, part ii: Event-based algorithm for networks. *Transportation Research Part B: Methodological*, 2018.
  21. J. Du, H. Rakha, and V. V. Gayah. Deriving macroscopic fundamental diagrams from probe data: Issues and proposed solutions. *Transportation Research Part C: Emerging Technologies*, 66:136–149, 2016.
  22. S. Fan, Y. Sun, B. Piccoli, B. Seibold, and D. B. Work. A Collapsed Generalized Aw-Rascle-Zhang Model and Its Model Accuracy. *ArXiv eprints*, Feb. 2017.
  23. A. K. Gupta & V. K. Katiyar, A New Multi-class Continuum Model For Traffic Flow, *Transportmetrica* Vol. 3, Iss. 1, 2007
  24. Liang Zheng, Peter J. Jin, Helai Huang, An anisotropic continuum model considering bi-directional information impact, *Transportation Research Part B: Methodological*, Volume 75, 2015, Pages 36-57, ISSN 0191-2615, <https://doi.org/10.1016/j.trb.2015.02.011>.
  25. Nagatani T. Bunching transition in a time-headway model of a bus route // *Phys. Rev. E*. 2001. Vol. 296, № 1-2. P.320-330.
  26. Regirer, S.A., Smirnov N.N., Chenchik, A.E. Mathematical model of moving collectives interaction: Public transport

- and passengers. *Automation and Remote Control*. 2007, vol. 68, No 7, pp. 1225-1238.
27. Sukhinova A.B., Trapeznikova M.A., Chetverushkin B.N., Churbanova N.G. Two dimensional macroscopic model for traffic flows. *Mathematical modeling*. 2009 vol. 21, #2, pp.118-126.
  28. Ngoduy, D. Application of gas-kinetic theory to modelling mixed traffic of manual and adaptive cruise control vehicles. *Transportmetrica Part A: Transport Science* **8**(1), 43–60(2012)
  29. Ngoduy, D. Platoon-based macroscopic model for intelligent traffic flow. *Transportmetrica B: Transport Dynamics*, **1**(2), 153–169(2013)
  30. Li, J. and Zhang, H.M. The variational formulation of a non-equilibrium traffic flow model: theory and implications. *Procedia - Social and Behavioral Sciences*, **80**, 327–340(2013)
  31. Zhu, Z.J. and Yang, C. Visco-elastic traffic flow model. *J. Advanced Transp.*, **47**, 635–649(2013)
  32. Tordeux, A., Roussignol, M., Lebacque, J.P. and Lassarre, S. A stochastic jump process applied to traffic flow modelling. *Transportmetrica A: Transport Science*, **10**(4), 350–375(2014)
  33. Costeseque, G. and Lebacque, J.P. A variational formulation for higher order macroscopic traffic flow models: Numerical investigation. *Transp. Res. Part B*, **70**, 112–133(2014)
  34. Bogdanova, A.I., Smirnova, M.N., Zhu, Z.J. and Smirnov, N.N. Exploring peculiarities of traffic flows with a viscoelastic model. *Transportmetrica A: Transport Science*, **11**(7), 561– 578(2015)
  35. Smirnova, M.N., Bogdanova, A.I., Zhu, Z.J., Smirnov, N.N. Traffic flow sensitivity to viscoelasticity. *Theoretical and Applied Mechanics Letters*, **6**, 182–185(2016)
  36. Smirnova, M.N., Bogdanova, A.I., Zhu, Z.J. and Smirnov, N.N. Traffic flow sensitivity to parameters in viscoelastic modelling. *Transportmetrica B: Transport Dynamics*, **5**(1), 115– 131(2017)
  37. Zhang, Y.L., Smirnova, M.N., Bogdanova, A.I., Zhu, Z.J. and Smirnov, N.N. Travel time estimation by urgent-gentle class traffic flow model. *Transp. Res. Part B* **113**, 121–142(2018)
  38. Kumar, B.A., Vanajakshi, L., Subramanian, S.C. Bus travel time prediction using a timespace discretization approach. *Transp. Res. Part C* **79**, 308–332(2017)
  39. Ladino, A., Kibangou, Y., Canudas de Wit, C., Fourati, H. Travel time prediction and departure time adjustment behavior dynamics in a congested traffic system. *Transp. Res. Part C* **80**, 216–238(2017)
  40. Ma, Z.L., Koutsopoulos, H.N., Ferreira, L., Mesbah, M. Estimation of trip travel time distribution using a generalized markov chain approach. *Transp. Res. Part C* **74**, 1–21(2017)
  41. Rahmani, M., Koutsopoulos, H.N., Jenelius, E. Travel time estimation from sparse floating car data with consistent path inference: a fixed point approach. *Transp. Res. Part C* **85**, 628–643(2017)
  42. Smirnov N.N. Kiselev A.B., Nikitin V.F., Yumashev M.V. Mathematical modelling of traffic flows. *Proc. 9<sup>th</sup> IFAC Symposium Control in Transportation Systems 2000, Braunschweig, 2000.*
  43. Kiselev A.B., Kokoreva A.V., Nikitin V.F., Smirnov N.N. Mathematical modeling of traffic flow dynamics. *Proc. of M.V.Lomonosov Conf. 2003, Moscow, p. 70.*
  44. John C. Tannehill, Dale A. Anderson, Richard H. Pletcher. *Computational fluid mechanics and heat transfer.* // Taylor & Frances, 1997. – 792 p.